Orientation relationships, orientational variants and the embedding approach

Richard Arnold,[a] Peter Jupp[b]* and Helmut Schaeben[c]

[a]School of Mathematics and Statistics, Victoria University of Wellington, PO Box 600, Wellington, New Zealand, [b]School of Mathematics and Statistics, University of St Andrews, North Haugh, St Andrews, Fife, KY16 9SS, United Kingdom, and [c]Geophysics and Geoscience Informatics, TU Bergakademie Freiberg, Freiberg, Germany. *Correspondence e-mail: pej@st-andrews.ac.uk

For phase transformations within polycrystalline materials, the connection between the crystal orientations of parent grains and those of child grains is usually expressed in terms of (theoretical or measured) orientation relationships. This paper introduces a new approach to various problems associated with orientation relationships: (i) estimation, (ii) whether or not a single orientation relationship fits the data adequately, (iii) whether or not a set of children comes from a common parent, and (iv) reconstruction of a parent or of grain boundaries. The approach is an extension to the crystallographic context of the well established embedding approach to directional statistics. It is inherently statistical, producing precise probabilistic statements. Explicit coordinate systems are not used and arbitrary thresholds are avoided.

1. Introduction

Phase transformations within polycrystalline materials often induce a transformation of the texture, *i.e.* of the statistical and spatial distribution of the crystallographic orientations of the crystallites. This usually involves the replacement of each parent crystal by several child crystals, possibly in a different symmetry group. Several mathematical models for describing these transformations have been constructed on theoretical grounds. Such models include the orientation relationships of Kurdjumow–Sachs (Kurdjumow & Sachs, 1930), Nishiyama–Wassermann (Wassermann, 1933, 1935; Nishiyama,1934) and Pitsch (1959, 1967). The presence of two symmetry groups leads to the problem of multiplicity of *variants*, *i.e.* orientations of (unseen) parent crystals giving rise to orientations of given child crystals. (A precise mathematical definition is given in Section 2.3.) Much work has been carried out developing methods for fitting these models and examining their adequacy, notably by Humbert and co-authors (*e.g.* Humbert *et al.*, 1994, 1995, 2015) and by Cayron and his collaborators (*e.g.* Cayron *et al.*, 2006; Cayron, 2019). Even within the topic of the austenite–martensite transformation there are very many papers in the materials science literature on problems involving variants, *e.g.* Nolze (2004*b*), Kitahara *et al.* (2006), Miyamoto *et al.* (2009), Abbasi *et al.* (2012, 2014), Koumatos & Muehlemann (2017) and Nyyssönen *et al.* (2016, 2018). These problems have been addressed by Mainprice *et al.* (1990) and Morales *et al.* (2018), for instance, in a geological context.

As far as we are aware, previous work on fitting orientation relationships and identifying variants takes the traditional viewpoint of estimating the relationship and assessing its fit, either informally or by making use of an arbitrary threshold of
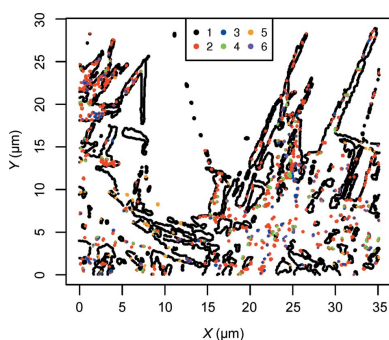
some measure of goodness of fit. For example, Nolze (2004*a*,*b*, 2005) measures the discrepancy between estimated and theoretical versions of a parameter $[\mathbf{A}]_{1,2}$ of an orientation relationship [see equation (1) below] by the (minimal) misorientation angle between representative rotations. The discrepancy is considered significant if it is larger than the accuracy of the experimental apparatus. In this paper we establish a sound statistical viewpoint on various types of problem involving orientation relationships and variants. In the traditional viewpoint, the key idea is that of being 'numerically close' and the typical question is 'how far apart are the measured and theoretical quantities?'. From the statistical viewpoint, the key idea is that of being 'statistically close' (in a precise probabilistic sense) and the typical question is 'what is the probability (under some hypothesis) that the measured and theoretical quantities are (at least) this far apart?'. If this probability is small then the hypothesis is rejected. We implement the statistical viewpoint here by using the embedding approach to crystallographic orientations introduced by Arnold *et al.* (2018), which is an application of the embedding approach to directional statistics [see *e.g.* Sections 2.1 and 9.1 of Mardia & Jupp (2000)]. The necessary measures of distance are constructed using orientation representations which incorporate the relevant symmetries, reducing the need to search for optimal representations within equivalence classes. The use of explicit coordinate systems is avoided.

The key points of our approach are as follows:

(i) Regarding each object such as a crystallographic orientation as a single object (equivalence class) in a quotient space, rather than considering a single representative orientation.

(ii) Avoiding arbitrary thresholds.

(iii) Avoiding arbitrarily chosen explicit coordinate systems (such as are used in asymmetric domains).

The notation used in this article is more mathematical and general than that traditionally used for discussing variants. The reasons for this choice are (i) the concepts of orientation relationship and variant are appropriate in contexts wider than the crystallographic, and (ii) for the embedding approach our notation is particularly convenient. We use the word 'random' in the statistical sense of 'not deterministic', so that repeating measurement of *e.g.* rotations will not produce exactly the same values (rather than implying that these rotations are uniformly distributed).

Some of the material in this paper has been presented in a more mathematical form suitable for statisticians by Arnold & Jupp (2019) and Arnold *et al.* (2018, 2021).

Section 2 gives a mathematical description of orientation relationships and variants. The embedding approach to crystallographic orientations is recalled in Section 3 and extended to the context of variants. Sections 4, 5, 6 and 7 treat methods for estimation (sometimes referred to as 'calculation', 'determination' or 'evaluation') of orientation relationships, assessment of the adequacy of a single orientation relationship, assessment of the common parentage of child crystals and reconstruction of parents, respectively. In each of these sections established methods are recalled and then methods based on the embedding approach are given. Some practical illustrations of these new methods are given in Section 8.

2. Orientation relationships and variants

2.1. Orientations of symmetrical objects

The orientation of a rigid object in $\mathbb{R}^3$ can be described by a rotation that transforms it into some standard orientation. If the object is asymmetrical then this rotation is unique, so that the orientations of the object correspond to elements of the group $SO(3)$ of rotations of $\mathbb{R}^3$. If the object has symmetry group K then a rotation $\mathbf{U}$ has the same effect as the rotation $\mathbf{UH}$ for any $\mathbf{H}$ in K. Then the orientations of the object correspond to elements of the space $SO(3)/K$, *i.e.* the set of equivalence classes of elements of $SO(3)$ under the right action of K. For $\mathbf{U}$ in $SO(3)$ we shall denote the corresponding left coset of K, *i.e.* the equivalence class $\{\mathbf{UH} : \mathbf{H} \in K\}$ of $\mathbf{U}$ in $SO(3)/K$ by $[\mathbf{U}]$.

2.2. Orientation relationships

In many contexts, *e.g.* transformations involving a phase change, interest lies in the relationship between two random orientations with possibly different symmetry groups. Let $[\mathbf{U}]_1$ and $[\mathbf{V}]_2$ be random orientations in $SO(3)/K_1$ and $SO(3)/K_2$, respectively, where K_1 and K_2 are the symmetry groups. Particularly simple models relating $[\mathbf{U}]_1$ and $[\mathbf{V}]_2$ are the *orientation relationships*. These have the form

$$[\mathbf{V}]_2 = [\mathbf{RUA}]_2, \tag{1}$$

where $\mathbf{R}$ and $\mathbf{A}$ are in $SO(3)$. {Note that, in general, equation (1) is not equivalent to $[\mathbf{U}]_1 = [\mathbf{R}^{-1}\mathbf{V}\mathbf{A}^{-1}]_1$.} The rotation $\mathbf{R}$ in (1) can arise as the result of measurements being made in different coordinate systems. For example, this situation arises when the two samples are aligned at different angles to a common laboratory measurement frame. A further complication may occur if pairs of measurements $([\mathbf{U}_1]_1, [\mathbf{V}_1]_2), \ldots, ([\mathbf{U}_n]_1, [\mathbf{V}_n]_2)$ are made at widely differing locations, in which case realistic modelling may require the use of an $\mathbf{R}$ that depends on location. Equation (1) determines the rotation $\mathbf{R}$ uniquely but it does not determine $\mathbf{A}$. Indeed, because $[\mathbf{U}]_1 = [\mathbf{UH}]_1$ and $[\mathbf{V}]_2 = [\mathbf{V}\widetilde{\mathbf{H}}]_2$ for any $\mathbf{H}$ in K_1 and any $\widetilde{\mathbf{H}}$ in K_2, $\mathbf{HA}\widetilde{\mathbf{H}}$ and $\mathbf{A}$ give the same orientation relationship (1). Thus (1) does not determine $\mathbf{A}$ fully but determines only its image $[\mathbf{A}]_{1,2}$ in the double coset space $K_1\backslash SO(3)/K_2$. The space $K_1\backslash SO(3)/K_2$ is the set of equivalence classes of elements $\mathbf{W}$ of $SO(3)$ for which $\mathbf{W}$ and $\mathbf{HW}\widetilde{\mathbf{H}}$ are equivalent for any $\mathbf{H}$ in K_1 and any $\widetilde{\mathbf{H}}$ in K_2. In crystallography it is usual to identify $K_1\backslash SO(3)/K_2$ with an asymmetric domain, *i.e.* a connected subset of $SO(3)$ that (apart from a set of measure zero) contains exactly one rotation in each equivalence class. Construction of asymmetric domains is considered in Section 6.3 of Morawiec (2004). Because, in any given context, there is no standard asymmetric domain, we prefer not to use such domains. An orientation relationship (1) gives rise to four types of problem:

(i) The *estimation problem* of estimating the unknown $\mathbf{R}$ and $[\mathbf{A}]_{1,2}$ on the basis of observations $([\mathbf{U}_1]_1, [\mathbf{V}_1]_2), \ldots, ([\mathbf{U}_n]_1, [\mathbf{V}_n]_2)$.

(ii) The *single orientation relationship problem* of assessing whether or not a single orientation relationship can describe the data adequately.

(iii) The *sibling problem* of determining whether or not elements $[\mathbf{V}_1]_2, \ldots, [\mathbf{V}_n]_2$ of $SO(3)/K_2$ arise from some unknown common parent $[\mathbf{U}]_1$ under a known orientation relationship $(\mathbf{R}, [\mathbf{A}]_{1,2})$. If $[\mathbf{V}_1]_2, \ldots, [\mathbf{V}_n]_2$ are distinct then they arise from some common $\mathbf{U}$ if and only if they are part of a set of variants (see Section 2.3).

(iv) The *reconstruction problem* of estimating the unknown $[\mathbf{U}]_1$ on the basis of a known $(\mathbf{R}, [\mathbf{A}]_{1,2})$ and observations $[\mathbf{V}_1]_2, \ldots, [\mathbf{V}_n]_2$.

These problems are considered in Sections 4, 5, 6 and 7, respectively.

2.3. Variants

In general, an orientation relationship (1) does not yield a unique map from $SO(3)/K_1$ to $SO(3)/K_2$. Instead, to each $[\mathbf{U}]_1$ in $SO(3)/K_1$ it assigns s distinct elements

$$[\mathbf{RUH}_1\mathbf{A}]_2, \ldots, [\mathbf{RUH}_s\mathbf{A}]_2, \qquad (2)$$

of $SO(3)/K_2$, where $\mathbf{H}_1, \ldots, \mathbf{H}_s \in K_1$ and

$$s = |K_1|/|K_\mathbf{A}|, \qquad (3)$$

$K_\mathbf{A}$ being the *intersection group* defined as

$$K_\mathbf{A} = K_1 \cap \left(\mathbf{A}K_2\mathbf{A}^{-1}\right). \qquad (4)$$

Distinctness of $[\mathbf{RUH}_1\mathbf{A}]_2, \ldots, [\mathbf{RUH}_s\mathbf{A}]_2$ in (2) is equivalent to $\mathbf{H}_j^{-1}\mathbf{H}_i \notin K_\mathbf{A}$ for $i \neq j$ (see Appendix *A*). The $[\mathbf{RUH}_1\mathbf{A}]_2, \ldots, [\mathbf{RUH}_s\mathbf{A}]_2$ in (2) are known as the (*orientation*) variants (or *crystallographic* variants) of $[\mathbf{U}]_1$ given by $\mathbf{R}$ and $\mathbf{A}$. There is no distinguished variant among $[\mathbf{RUH}_1\mathbf{A}]_2, \ldots, [\mathbf{RUH}_s\mathbf{A}]_2$, but the (arbitrary) choice of any one of these, $[\mathbf{RUH}_0\mathbf{A}]_2$, say, as a base point determines the function $\phi_{\mathbf{H}_0}$ from K_1 to the set of variants by $\phi_{\mathbf{H}_0}([\mathbf{H}]_1) = [\mathbf{RUH}_0\mathbf{HA}]_2$. Since $\phi_{\mathbf{H}_0}([\mathbf{H}_i]_1) = \phi_{\mathbf{H}_0}([\mathbf{H}_j]_1)$ if and only if $\mathbf{H}_j^{-1}\mathbf{H}_i \in K_\mathbf{A}$, the set (2) of variants can be identified with the coset space $K_1/K_\mathbf{A}$.

As pointed out by Nolze (2008), in contrast to the commonly used theoretical orientation relationships $[\mathbf{A}]_{1,2}$, measured orientation relationships $[\widehat{\mathbf{A}}]_{1,2}$ are 'irrational' in that their descriptions in terms of crystallographic planes and directions do not have low Miller indices. This is because it is not possible to make measurements with perfect accuracy, and so the orientations $[\mathbf{U}_i]_1$ and $[\mathbf{V}_i]_2$ are random. The argument in Proposition 1 in Appendix *A* shows that the number of variants associated with a measured orientation relationship is $|K_1|$. In real materials the variants are usually present in unequal quantities, a phenomenon known as *variant selection*, and some variants may even be absent. In many contexts it is of interest to estimate the overall proportions of the variants that are present. Whereas the orientational variants considered in this paper are cosets of $K_\mathbf{A}$ in K_1, the types of variant introduced by Cayron (2016, 2019) in connection with the

physical mechanisms underlying martensitic crystallography are cosets of other subgroups of K_1 that describe the distortion and stretch of crystal lattices.

As pointed out by Cayron (2006), the important algebraic structure associated with the set (2) of variants is that of a groupoid, *i.e.* a set of arrows endowed with a partially defined associative composition in which every arrow has an inverse. Denote the set (2) of variants by V. Each triple $([\mathbf{RUH}_i\mathbf{A}]_2, K_\mathbf{A}\mathbf{H}_i^{-1}\mathbf{H}_jK_\mathbf{A}, [\mathbf{RUH}_j\mathbf{A}]_2)$ in $V \times (K_\mathbf{A}\backslash K_1/K_\mathbf{A}) \times V$ can be regarded as an arrow from $[\mathbf{RUH}_i\mathbf{A}]_2$ to $[\mathbf{RUH}_j\mathbf{A}]_2$. The arrows $([\mathbf{RUH}_i\mathbf{A}]_2, K_\mathbf{A}\mathbf{H}_i^{-1}\mathbf{H}_jK_\mathbf{A}, [\mathbf{RUH}_j\mathbf{A}]_2)$ and $([\mathbf{RUH}_k\mathbf{A}]_2, K_\mathbf{A}\mathbf{H}_k^{-1}\mathbf{H}_\ell K_\mathbf{A}, [\mathbf{RUH}_\ell\mathbf{A}]_2)$ can be composed if and only if $[\mathbf{RUH}_j\mathbf{A}]_2 = [\mathbf{RUH}_k\mathbf{A}]_2$, in which case the composition is $([\mathbf{RUH}_i\mathbf{A}]_2, K_\mathbf{A}\mathbf{H}_\ell^{-1}\mathbf{H}_kK_\mathbf{A}, [\mathbf{RUH}_\ell\mathbf{A}]_2)$. It is useful to combine the arrows into equivalence classes called *operators*. Each operator can be written as $K_\mathbf{A}\mathbf{H}_i^{-1}\mathbf{H}_jK_\mathbf{A}$ for some i, j (but, in general, i and j are not unique) and can be regarded as being a theoretical transformation that takes the variant $[\mathbf{RUH}_i\mathbf{A}]_2$ to $[\mathbf{RUH}_j\mathbf{A}]_2$. Thus, the set of operators can be identified with the double coset space $K_\mathbf{A}\backslash K_1/K_\mathbf{A}$. The operator $K_\mathbf{A}\mathbf{H}_i^{-1}\mathbf{H}_jK_\mathbf{A}$ can be regarded as the misorientation between $[\mathbf{RUH}_i\mathbf{A}]_2$ and $[\mathbf{RUH}_j\mathbf{A}]_2$.

The composition table of the groupoid yields a multi-valued composition on the set of operators. This provides a way of attacking the sibling and reconstruction problems described in points (iii) and (iv) at the end of Section 2.2. Gey & Humbert (2003) pointed out that, in the case of the Burgers orientation relationship $(K_1 = O, K_2 = D_6)$, the number of misorientations between the variants is less than the number of variants.

3. The embedding approach

3.1. Embedding $SO(3)/K$

Because the coset spaces $SO(3)/K$ are not very easy to work with, Arnold *et al.* (2018) (see also Arnold & Jupp, 2019) developed the *embedding approach* in which a function $\mathbf{t} : SO(3)/K \rightarrow E$ is used to send $SO(3)/K$ into (but not onto) some inner-product space E. The function $\mathbf{t}$ is required to be (i) one-to-one, (ii) equivariant, *i.e.* $\langle \mathbf{t}([\mathbf{VU}]), \mathbf{t}([\mathbf{VW}]) \rangle = \langle \mathbf{t}([\mathbf{U}]), \mathbf{t}([\mathbf{W}]) \rangle$ for $\mathbf{U}, \mathbf{V}, \mathbf{W}$ in $SO(3)$, where $\langle \cdot, \cdot \rangle$ denotes the inner product, (iii) such that $\mathbf{t}([\mathbf{U}])$ has expectation 0 if $[\mathbf{U}]$ is uniformly distributed on $SO(3)/K$. For the crystallographic groups $C_1, C_2, C_3, C_4, D_2, D_6, T$ and O some useful functions $\mathbf{t}$ are given explicitly in Table 1. Together $\mathbf{t}$ and $\langle \cdot, \cdot \rangle$ lead us to

$$\|\mathbf{t}([\mathbf{U}]) - \mathbf{t}([\mathbf{V}])\|^2 = \langle \mathbf{t}([\mathbf{U}]) - \mathbf{t}([\mathbf{V}]), \mathbf{t}([\mathbf{U}]) - \mathbf{t}([\mathbf{V}]) \rangle \quad (5)$$

as a new measure of squared distance between elements $[\mathbf{U}]$ and $[\mathbf{V}]$ of $SO(3)/K$. By design it incorporates the symmetry group K and it replaces the need for misorientation angles. A useful summary of $[\mathbf{U}_1], \ldots, [\mathbf{U}_n]$ is their *sample mean*, $[\overline{\mathbf{U}}]$, which is defined as the element of $SO(3)/K$ that minimizes $\sum_{i=1}^{n} \|\mathbf{t}([\overline{\mathbf{U}}]) - \mathbf{t}([\mathbf{U}_i])\|^2$ or, equivalently, maximizes $\langle \mathbf{t}([\overline{\mathbf{U}}]), \sum_{i=1}^{n} \mathbf{t}([\mathbf{U}_i]) \rangle$. For $K = C_r$ or D_r explicit approximations to sample means are given in Section 2.3 of Arnold & Jupp (2019).

Embeddings are discussed further in Appendix *B*.

Table 1
Some embeddings $\mathbf{t}_K : SO(3)/K \to E$.

For C_r with $r \geq 3$, $\mathbf{u}_0 = [\sin(2\pi/r)]^{-1} \mathbf{u}_1 \times \mathbf{u}_2$. For D_2, $\mathbf{u}_3 = \pm\mathbf{u}_1 \times \mathbf{u}_2$. The symmetric arrays $\otimes^r\mathbf{u}_i$ and $\mathbf{N}_r$ are defined in equations (37) and (38), respectively.

Group, K	$\mathbf{t}_K$
C_1	$\mathbf{t}_{C_1}(\mathbf{u}_1, \mathbf{u}_2, \mathbf{u}_3) = (\mathbf{u}_1, \mathbf{u}_2, \mathbf{u}_3)$
C_2	$\mathbf{t}_{C_2}(\mathbf{u}_0, \pm\mathbf{u}_1) = (\mathbf{u}_0, \mathbf{u}_1\mathbf{u}_1^T - \frac{1}{3}\mathbf{I}_3)$
C_3	$\mathbf{t}_{C_3}([\mathbf{u}_1, \mathbf{u}_2, \mathbf{u}_3]) = \left(\mathbf{u}_0, \sum_{i=1}^{3} \otimes^3\mathbf{u}_i\right)$
C_4	$\mathbf{t}_{C_4}([\mathbf{u}_1, \ldots, \mathbf{u}_4]) = \left(\mathbf{u}_0, \sum_{i=1}^{4} \otimes^4\mathbf{u}_i - \frac{4}{5}\mathbf{N}_4\right)$
D_2	$\mathbf{t}_{D_2}(\pm\mathbf{u}_1, \pm\mathbf{u}_2) = (\mathbf{u}_1\mathbf{u}_1^T - \frac{1}{3}\mathbf{I}_3, \mathbf{u}_2\mathbf{u}_2^T - \frac{1}{3}\mathbf{I}_3, \mathbf{u}_3\mathbf{u}_3^T - \frac{1}{3}\mathbf{I}_3)$
D_4	$\mathbf{t}_{D_4}([\mathbf{u}_1, \ldots, \mathbf{u}_4]) = \sum_{i=1}^{4} \otimes^4\mathbf{u}_i - \frac{4}{5}\mathbf{N}_4$
D_6	$\mathbf{t}_{D_6}([\mathbf{u}_1, \ldots, \mathbf{u}_6]) = \sum_{i=1}^{6} \otimes^6\mathbf{u}_i - \frac{6}{7}\mathbf{N}_6$
T	$\mathbf{t}_T(\{u_1, \mathbf{u}_2, \mathbf{u}_3, \mathbf{u}_4\}) = \otimes^3\mathbf{u}_1 + \otimes^3\mathbf{u}_2 + \otimes^3\mathbf{u}_3 + \otimes^3\mathbf{u}_4$
O	$\mathbf{t}_O(\{\pm\mathbf{u}_1, \pm\mathbf{u}_2, \pm\mathbf{u}_3\}) = \otimes^4\mathbf{u}_1 + \otimes^4\mathbf{u}_2 + \otimes^4\mathbf{u}_3 - \frac{3}{5}\mathbf{N}_4$

3.2. Embedding $K_1\backslash SO(3)/K_2$

The double coset spaces $K_1\backslash SO(3)/K_2$ are even more complicated than the coset spaces $SO(3)/K$, but the embedding approach can be used for them also.

Any $\mathbf{t} : SO(3)/K_2 \to E$, where E is a vector space, can be averaged over K_1 to give a corresponding $\bar{\mathbf{t}} : K_1\backslash SO(3)/K_2 \to E$, defined by

$$\bar{\mathbf{t}}([\mathbf{U}]_{1,2}) = |K_1|^{-1} \sum_{\mathbf{H} \in K_1} \mathbf{t}([\mathbf{HU}]_2). \qquad (6)$$

We shall exploit such $\bar{\mathbf{t}}$ in order to carry out inference on orientation relationships. If $\mathbf{t}$ has properties (ii) and (iii) of Section 3.1 then so does $\bar{\mathbf{t}}$. On the other hand, $\mathbf{t}$ having property (i) (being one-to-one) does not imply that $\bar{\mathbf{t}}$ has this property also. In a few very special cases (*e.g.* K_1 and K_2 isomorphic to C_2 and C_3 and with a common axis) $\bar{\mathbf{t}}$ is identically zero. In the context of phase transitions it seems that such symmetries are not of practical interest.

4. Estimation

4.1. Estimation based on orientations of parents and children: established methods

Suppose that we are given paired observations $([\mathbf{U}_1]_1, [\mathbf{V}_1]_2), \ldots, ([\mathbf{U}_n]_1, [\mathbf{V}_n]_2)$ with $[\mathbf{U}_i]_1$ in $SO(3)/K_1$ and $[\mathbf{V}_i]_2$ in $SO(3)/K_2$ for $1 \leq i \leq n$. It is assumed that the pairs $([\mathbf{U}_1]_1, [\mathbf{V}_1]_2), \ldots, ([\mathbf{U}_n]_1, [\mathbf{V}_n]_2)$ are observations of a pair $([\mathbf{U}]_1, [\mathbf{V}]_2)$

of random orientations that satisfy the orientation relationship (1). The problem is that of estimating the unknown $[\mathbf{A}]_{1,2}$ (and $\mathbf{R}$ if it is not known). In the case $K_1 = K_2 = C_1$ (*i.e.* no symmetry, so that variants do not occur), an explicit estimate of $\mathbf{A}$ was given by Mackenzie (1957). In the general case, it follows from (1) that $[\mathbf{U}_i^{-1}\mathbf{R}^{-1}\mathbf{V}_i]_{1,2}$ is close to $[\mathbf{A}]_{1,2}$ for $i = 1, \ldots, n$. Then $[\mathbf{U}_i^{-1}\mathbf{R}^{-1}\mathbf{V}_i]_{1,2}$ can be considered as the 'local' estimate of $[\mathbf{A}]_{1,2}$ given by the observed pair $([\mathbf{U}_i]_1, [\mathbf{V}_i]_2)$. Here 'local' is used in the sense that the estimate uses only quantities with index i, which in many cases means that they are measured at the ith location.

Using this approach Nolze found that, for transformation from face-centred cubic to body-centred cubic lattices, the standard theoretical models did not provide a good fit to the experimental data that he was investigating

4.2. Estimation based on orientations of parents and children: embedding approach

The embedding approach uses a suitable embedding $\mathbf{t}_2 : SO(3)/K_2 \to E$. If $([\mathbf{U}_1]_1, [\mathbf{V}_1]_2), \ldots, ([\mathbf{U}_n]_1, [\mathbf{V}_n]_2)$ are observations on a pair $([\mathbf{U}]_1, [\mathbf{V}]_2)$ of random orientations that satisfy the orientation relationship (1) then $[\mathbf{U}_i^{-1}\mathbf{R}^{-1}\mathbf{V}_i]_{1,2}$ is close to $[\mathbf{A}]_{1,2}$ for $i = 1, \ldots, n$. Therefore, it is sensible to estimate $\mathbf{R}$ and $[\mathbf{A}]_{1,2}$ by $\widehat{\mathbf{R}}$ and $[\widehat{\mathbf{A}}]_{1,2}$, which are the $\mathbf{R}$ and $[\mathbf{A}]_{1,2}$ that minimize the squared distance $\sum_{i=1}^{n} \|\bar{\mathbf{t}}_2([\mathbf{U}_i^{-1}\mathbf{R}^{-1}\mathbf{V}_i]_{1,2}) - \bar{\mathbf{t}}_2([\mathbf{A}]_{1,2})\|^2$, or equivalently that maximize $S_2(\mathbf{R}, [\mathbf{A}]_{1,2}; \{([\mathbf{U}_i]_1, [\mathbf{V}_i]_2)\}_{i=1}^{n})$, defined by

$$S_2\big(\mathbf{R}, [\mathbf{A}]_{1,2}; \big\{([\mathbf{U}_i]_1, [\mathbf{V}_i]_2)\big\}_{i=1}^{n}\big)$$
$$= \sum_{i=1}^{n} \big\langle \bar{\mathbf{t}}_2([\mathbf{A}]_{1,2}), \bar{\mathbf{t}}_2([\mathbf{U}_i^{-1}\mathbf{R}^{-1}\mathbf{V}_i]_{1,2}) \big\rangle$$
$$= n\left\langle \mathbf{t}_2([\mathbf{A}]_2), \frac{1}{n|K_1|} \sum_{i=1}^{n} \sum_{\mathbf{H} \in K_1} \mathbf{t}_2([\mathbf{HU}_i^{-1}\mathbf{R}^{-1}\mathbf{V}_i]_2) \right\rangle. \qquad (7)$$

Thus, $[\mathbf{A}]_{1,2}$ can be taken as the sample mean of the images by $\bar{\mathbf{t}}_2$ [defined by (6)] of $\{[\mathbf{HU}_i^{-1}\mathbf{R}^{-1}\mathbf{V}_i]_2 : \mathbf{H} \in K_1, i = 1, \ldots, n\}$. An alternative method of estimation uses the $\mathbf{R}$ and $[\mathbf{A}]_{1,2}$ that maximize $S_\infty(\mathbf{R}, [\mathbf{A}]_{1,2}; \{([\mathbf{U}_i]_1, [\mathbf{V}_i]_2)\}_{i=1}^{n})$, which is defined by

$$S_\infty(\mathbf{R}, [\mathbf{A}]_{1,2}; \{([\mathbf{U}_i]_1, [\mathbf{V}_i]_2)\}_{i=1}^{n})$$
$$= \sum_{i=1}^{n} \max_{\mathbf{H} \in K_1} \langle \mathbf{t}_2([\mathbf{HA}]_2), \mathbf{t}_2([\mathbf{U}_i^{-1}\mathbf{R}^{-1}\mathbf{V}_i]_2) \rangle \qquad (8)$$

[see Section 6.1 of Arnold *et al.* (2021)].

Not only can a point estimate $[\widehat{\mathbf{A}}]_{1,2}$ of $[\mathbf{A}]_{1,2}$ be obtained, it is also possible to get confidence regions for $[\mathbf{A}]_{1,2}$. Bootstrap confidence regions for $[\mathbf{A}]_{1,2}$ can be calculated by resampling the data as follows. For a suitable B and m, for $b = 1, \ldots, B$, sample (with replacement) m pairs ($m \leq n$) $([\mathbf{U}_{b1}]_1, [\mathbf{V}_{b1}]_2), \ldots, ([\mathbf{U}_{bm}]_1, [\mathbf{V}_{bm}]_2)$ from $([\mathbf{U}_1]_1, [\mathbf{V}_1]_2), \ldots, ([\mathbf{U}_n]_1, [\mathbf{V}_n]_2)$. Denote the estimate of $[\mathbf{A}]_{1,2}$ based on $([\mathbf{U}_{b1}]_1, [\mathbf{V}_{b1}]_2), \ldots, ([\mathbf{U}_{bm}]_1, [\mathbf{V}_{bm}]_2)$ by $[\widehat{\mathbf{A}}_b]_{1,2}$. Define the similarity measure

$$\delta([\mathbf{A}]_{1,2}, [\mathbf{B}]_{1,2}) = \max_{\mathbf{H} \in K_1} \langle \mathbf{t}_2([\mathbf{HA}]_{1,2}), \mathbf{t}_2([\mathbf{B}]_{1,2}) \rangle. \qquad (9)$$

For $0 < \alpha < 1$, define c_α by
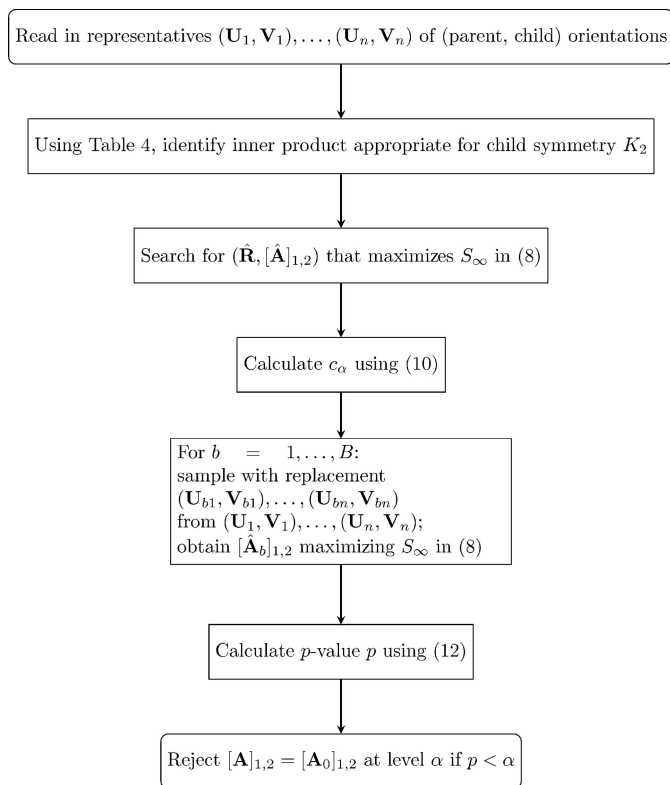
Figure 1
A flow chart for (i) estimation of $(\mathbf{R}, [\mathbf{A}_{1,2}])$ based on $(\mathbf{U}_1, \mathbf{V}_1), \ldots, (\mathbf{U}_n, \mathbf{V}_n)$, (ii) confidence regions for $[\mathbf{A}_{1,2}]$ and (iii) testing of $[\mathbf{A}_{1,2}] = [\mathbf{A}_{01,2}]$. An alternative method minimizes S_2 in (7) instead of S_∞ in (8).

$$c_\alpha = 100 \times (1 - \alpha)\% \text{ largest of } \left\{ \delta([\widehat{\mathbf{A}}_b]_{1,2}, [\widehat{\mathbf{A}}]_{1,2}) \right\}_{b=1}^{B}. \quad (10)$$

Then a $100 \times (1 - \alpha)\%$ bootstrap confidence region for $[\mathbf{A}]_{1,2}$ is

$$\left\{ [\mathbf{A}]_{1,2} : \delta([\mathbf{A}]_{1,2}, [\widehat{\mathbf{A}}]_{1,2}) > c_\alpha \right\}. \quad (11)$$

For the corresponding test of $H_0 : [\mathbf{A}]_{1,2} = [\mathbf{A}_0]_{1,2}$ (where $[\mathbf{A}_0]_{1,2}$ is a specified theoretical $[\mathbf{A}]_{1,2}$), the p-value (*i.e.* the probability under H_0 of another sample producing a value of $[\widehat{\mathbf{A}}]_{1,2}$ at least as extreme as that observed) is

$$p = B^{-1} \text{ No. of } \left\{ b : \delta([\widehat{\mathbf{A}}_b]_{1,2}, [\widehat{\mathbf{A}}]_{1,2}) > \delta([\mathbf{A}_0]_{1,2}, [\widehat{\mathbf{A}}]_{1,2}) \right\}. \quad (12)$$

The hypothesis H_0 is rejected at significance level α if $p \leq \alpha$ or, equivalently, if the estimated $[\widehat{\mathbf{A}}]_{1,2}$ lies outside the $100 \times (1 - \alpha)\%$ bootstrap confidence region (11) for $[\mathbf{A}]_{1,2}$.

A flow chart for implementation of the techniques described in this subsection is given in Fig. 1.

4.3. Estimation based on orientations of children alone: established methods

In some settings, no observations on the orientations of parent grains are available. Nevertheless, in many cases it is possible to estimate $[\mathbf{A}]_{1,2}$ from orientations $[\mathbf{V}_1]_2, \ldots, [\mathbf{V}_n]_2$ of child grains.

The estimation method of Humbert *et al.* (2015) starts from observed child crystallographic orientations $[\mathbf{V}_1]_2, \ldots, [\mathbf{V}_3]_2$ that are the visible part of $([\mathbf{U}_1]_1, [\mathbf{V}_1]_2), ([\mathbf{U}_2]_1, [\mathbf{V}_2]_2), ([\mathbf{U}_3]_1, [\mathbf{V}_3]_2)$. These pairs are taken to obey (at least approximately) a form of the orientation relationship (1), so that

$$[\mathbf{V}_r]_2 \simeq [\mathbf{RU}_r\mathbf{A}_r]_2, \quad r = 1, 2, 3 \quad (13)$$

for some $\mathbf{U}_1, \mathbf{U}_2, \mathbf{U}_3$ and $\mathbf{A}_1, \mathbf{A}_2, \mathbf{A}_3$. It is assumed that $\mathbf{U}_1 \simeq \mathbf{U}_2 \simeq \mathbf{U}_3 \simeq \mathbf{U}$ and $\mathbf{A}_1 \simeq \mathbf{A}_2 \simeq \mathbf{A}_3 \simeq \mathbf{A}$ for some $\mathbf{U}$ and $\mathbf{A}$ in $SO(3)$ (assumptions that are reasonable if the orientations are measured at points near a triple junction and the local orientation relationships vary only slowly with position). It then follows from (13) that for i, j in $\{1, 2, 3\}$ it is possible to choose $\mathbf{H}_i, \mathbf{H}_j$ in K_1 and $\widetilde{\mathbf{H}}_i, \widetilde{\mathbf{H}}_j$ in K_2 such that $\mathbf{U}_i \simeq \mathbf{UH}_i, \mathbf{U}_j \simeq \mathbf{UH}_j$ and

$$\mathbf{V}_i \simeq \mathbf{RUH}_i\mathbf{A}\widetilde{\mathbf{H}}_i, \quad \mathbf{V}_j \simeq \mathbf{RUH}_j\mathbf{A}\widetilde{\mathbf{H}}_j. \quad (14)$$

Then

$$\mathbf{V}_j^{-1}\mathbf{V}_i \simeq \widetilde{\mathbf{H}}_j^{-1}\mathbf{A}^{-1}\mathbf{H}_j^{-1}\mathbf{H}_i\mathbf{A}\widetilde{\mathbf{H}}_i \quad (15)$$

or, equivalently,

$$\mathbf{A}\widetilde{\mathbf{H}}_j\mathbf{V}_i^{-1}\mathbf{V}_j \simeq \mathbf{H}_m\mathbf{A}\widetilde{\mathbf{H}}_i, \quad (16)$$

where $\mathbf{H}_m = \mathbf{H}_j^{-1}\mathbf{H}_i$. For given i and j, solutions for $\mathbf{A}$ of the equation obtained from (16) by replacing approximate equality by exact equality are far from unique. On the other hand, for general $\mathbf{V}_1, \mathbf{V}_2, \mathbf{V}_3$ (outside some set of measure 0), the three corresponding equations as i, j run through distinct (unordered) pairs in $\{1, 2, 3\}$ do have a unique solution. In view of this, Humbert *et al.* (2015) suggested estimating the rotation $\mathbf{A}$ by any element of $SO(3)$ that minimizes

$$\sum_{(i,j)} \min_{\mathbf{H}_m \in K_1} \min_{\widetilde{\mathbf{H}}_i, \widetilde{\mathbf{H}}_j \in K_2} \|\mathbf{A}\widetilde{\mathbf{H}}_j\mathbf{V}_j^{-1}\mathbf{V}_i - \mathbf{H}_m\mathbf{A}\widetilde{\mathbf{H}}_i\|^2, \quad (17)$$

the sum being over $(i, j) = (1, 2), (1, 3), (2, 3)$ and the norm being the Frobenius norm [= Hilbert–Schmidt norm, defined by $\|\mathbf{B}\|^2 = \text{trace}(\mathbf{BB}^{\mathrm{T}})$].

The estimation stage of the iterative reconstruction method of Nyyssönen *et al.* (2016, 2018) is also motivated by (16). Given (i) orientations $[\mathbf{V}_i]_2$ and $[\mathbf{V}_j]_2$ of distinct variants and (ii) $\mathbf{H}_m$ in K_1 and $\widetilde{\mathbf{H}}_i, \widetilde{\mathbf{H}}_j$ in K_2, $[\mathbf{A}]_{1,2}$ is estimated by $[\widehat{\mathbf{A}}]_{1,2}$, where $\widehat{\mathbf{A}}$ is found by iterative solution of

$$\mathbf{A} = \mathbf{H}_m\mathbf{A}\widetilde{\mathbf{H}}_i\mathbf{V}_i^{-1}\mathbf{V}_j\widetilde{\mathbf{H}}_j^{-1}. \quad (18)$$

Since $\mathbf{H}_m, \widetilde{\mathbf{H}}_i$ and $\widetilde{\mathbf{H}}_j$ are not known, Nyyssönen and co-workers recommend averaging the above $\widehat{\mathbf{A}}$ as $\mathbf{H}_m, \widetilde{\mathbf{H}}_i, \widetilde{\mathbf{H}}_j$ run through K_1, K_2, K_2. Note that averaging of rotations is not well defined.

4.4. Estimation based on orientations of children alone: embedding approach

Given an embedding $\mathbf{t}_2 : SO(3)/K_2 \rightarrow E$, define $\check{\mathbf{t}}_2 : K_2 \backslash SO(3)/K_2 \rightarrow E$ by

research papers
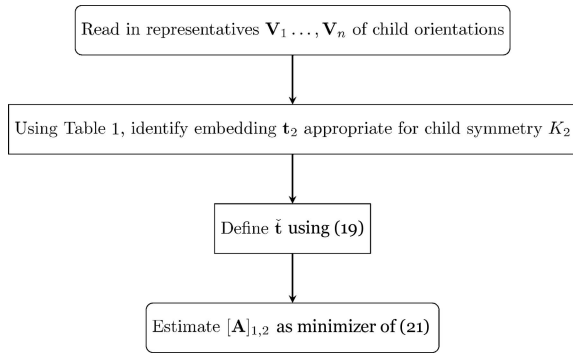
Figure 2
A flow chart for estimation of $[\mathbf{A}_{1,2}]$ based on $\mathbf{V}_1, \ldots \mathbf{V}_n$.

$$\check{\mathbf{t}}_2([\mathbf{V}]_{2,2}) = |K_2|^{-1} \sum_{\widetilde{\mathbf{H}} \in K_2} \mathbf{t}_2([\widetilde{\mathbf{H}}\mathbf{V}]_2), \qquad (19)$$

where $[\mathbf{V}]_{2,2}$ denotes the image of $[\mathbf{V}]_2$ in the double coset space $K_2 \backslash SO(3)/K_2$.

It follows from (15) that

$$\check{\mathbf{t}}_2(\mathbf{V}_i^{-1}\mathbf{V}_j) \simeq \check{\mathbf{t}}_2(\mathbf{A}^{-1}\mathbf{H}_m\mathbf{A}) \qquad (20)$$

for some $\mathbf{H}_m$ in K_1. It is therefore reasonable to estimate $[\mathbf{A}]_{1,2}$ as any element of $K_1 \backslash SO(3)/K_2$ that minimizes

$$\sum_{(i,j)} \min_{\mathbf{H}_m \in K_1} \|\check{\mathbf{t}}_2(\mathbf{V}_i^{-1}\mathbf{V}_j) - \check{\mathbf{t}}_2(\mathbf{A}^{-1}\mathbf{H}_m\mathbf{A})\|^2, \qquad (21)$$

the sum being over ordered pairs (i, j) of distinct elements of $\{1, \ldots, n\}$.

A flow chart for implementation of the technique described in this subsection is given in Fig. 2.

5. Assessing the adequacy of a single orientation relationship

Whereas some data sets can be fitted well by the orientation relationship (1), for others such a single orientation relationship is inadequate and several orientation relationships are required. For data sets in which a single orientation relationship does not suffice, it is possible to identify clusters of observations within each of which the data share a single orientation relationship.

5.1. Established methods

We are unaware of anything in the crystallographic literature that considers exactly this problem.

5.2. Embedding approach

One way of exploring the adequacy of (1) is to use cluster analysis to divide the n pairs of observations $([\mathbf{U}_1]_1, [\mathbf{V}_1]_2), \ldots, ([\mathbf{U}_n]_1, [\mathbf{V}_n]_2)$ into subsets, each of which consists of pairs that give similar estimates of $[\mathbf{A}]_{1,2}$. Cluster analysis is described in detail by Everitt *et al.* (2011), who give several algorithms. We find it convenient to use the following simple divisive algorithm. For an estimate $[\widehat{\mathbf{A}}]_{1,2}$ found using the method of Section 4.2 and for $i = 1, \ldots, n$, define d_i by

Table 2
Values of the squared radius ρ^2.

ρ^2 is defined in equation (23).

Group, K	ρ^2
C_1	3
C_2	5/3
C_r ($r \geq 3$)	
r odd	$1 + 2^{1-r}r^2$
r even	$1 + r^2 2^{1-r}\{1 + 2^{-1}\binom{r}{r/2}\} - r^2/(r+1)$
D_2	2
D_r ($r \geq 3$)	
r odd	$2^{1-r}r^2$
r even	$r^2 2^{1-r}\{1 + 2^{-1}\binom{r}{r/2}\} - r^2/(r+1)$
T	32/9
O	6/5

$$d_i = \delta([\mathbf{U}_i^{-1}\mathbf{V}_i]_{1,2}, [\widehat{\mathbf{A}}]_{1,2}), \qquad (22)$$

where δ is defined in (9). The maximum possible value of d_i is

$$\rho^2 = \langle \mathbf{t}_2([\mathbf{U}]_2), \mathbf{t}_2([\mathbf{U}]_2)\rangle \qquad (23)$$

[which does not depend on $\mathbf{U}$ in $SO(3)$]. A value of d_i near ρ^2 indicates that the 'local estimate' $[\mathbf{U}_i^{-1}\mathbf{V}_i]_{1,2}$ of $[\mathbf{A}]_{1,2}$ is close to the 'global estimate' $[\widehat{\mathbf{A}}]_{1,2}$. The values of ρ^2 corresponding to various symmetry groups are given in Table 2. If the single orientation relationship $[\widehat{\mathbf{A}}]_{1,2}$ gives a good fit to the data $([\mathbf{U}_1]_1, [\mathbf{V}_1]_2), \ldots, ([\mathbf{U}_n]_1, [\mathbf{V}_n]_2)$ then $d_1, \ldots, d_n$ are all large. Placing all observations with d_i close to ρ^2 into a cluster, re-estimate $[\widehat{\mathbf{A}}]_{1,2}$ for that cluster. Repeat this process on the remaining observations, thus grouping them sequentially into clusters having similar local orientation relationships. If only one cluster is found then the single orientation relationship $[\widehat{\mathbf{A}}]_{1,2}$ will describe the data well. Whereas the clustering of locations used by Johnstone *et al.* (2020) and Ostapovich & Trusov (2021) in the construction of crystal orientation maps takes place on $SO(3)/K$ and is based on misorientation angles, the clustering used here takes place on $K_1 \backslash SO(3)/K_2$ and is based on the d_i of (22). The clustering of locations used by Gomes de Araujo *et al.* (2021) in the reconstruction of parent microstructure is based on misorientation angles between adjacent grains.

A flow chart for implementation of the technique described in this subsection is given in Fig. 3.

6. Common parentage

In some contexts, such as locating the boundaries of parent grains, it is useful to be able to assess whether or not a set of child crystals are from the same parent. Observed elements $[\mathbf{V}_1]_2, \ldots, [\mathbf{V}_n]_2$ of $SO(3)/K_2$ can be considered as arising from some common parent if and only if they are close to variants corresponding to some element of $SO(3)/K_1$.

6.1. Established methods

The method of Gey & Humbert (2003) and Karthikeyan *et al.* (2006) assesses $[\mathbf{V}_1]_2, \ldots, [\mathbf{V}_n]_2$ to be from the same parent if the observed misorientation angles between $[\mathbf{V}_i]_2$ and $[\mathbf{V}_j]_2$ for $1 \leq i, j \leq n$ are within some given threshold of the theo-
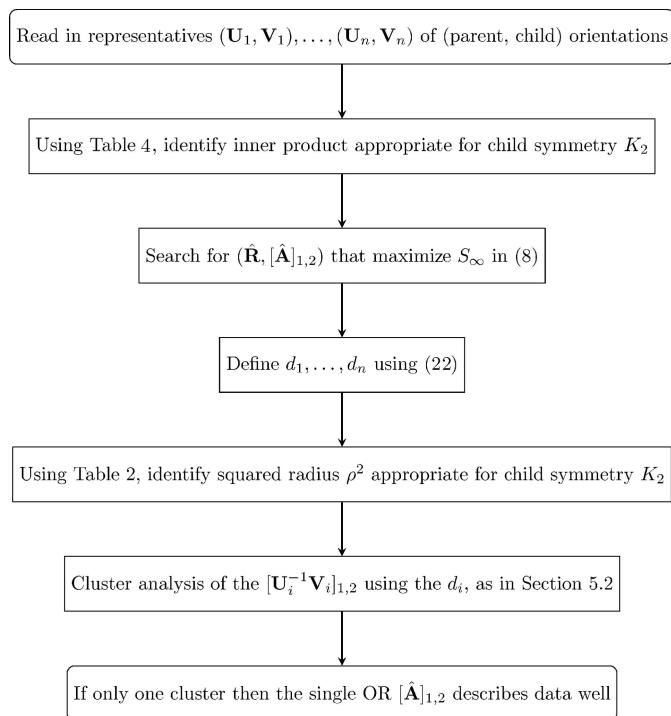
Figure 3
A flow chart for assessing the adequacy of a single orientation relationship (OR).

retical misorientation angles. These observed misorientation angles are

$$\arccos \left[\{ \max \operatorname{tr}(\widetilde{\mathbf{V}}_i^{-1} \widetilde{\mathbf{V}}_j) - 1 \} / 2 \right], \tag{24}$$

where the maximum is over $\widetilde{\mathbf{V}}_i$ in $SO(3)$ with $[\widetilde{\mathbf{V}}_i]_{1,2} = [\mathbf{V}_i]_{1,2}$ for $i = 1, \ldots, n$.

Cayron *et al.* (2006) considered the problem of finding maximal sets $[\mathbf{V}_1]_2, \ldots, [\mathbf{V}_n]_2$ of children from a common parent. Their method is based on considering triples $[\mathbf{V}_i]_2$, $[\mathbf{V}_j]_2$ and $[\mathbf{V}_k]_2$ to be from the same parent if they are *coherent*, *i.e.* there are operators O_{ij}, O_{ik}, O_{jk} taking $[\mathbf{V}_i]_2$ to $[\mathbf{V}_j]_2$, $[\mathbf{V}_i]_2$ to $[\mathbf{V}_k]_2$, $[\mathbf{V}_j]_2$ to $[\mathbf{V}_k]_2$, respectively, (at least approximately) and with O_{ik} as some value of the composition of O_{jk} with O_{ij}. Such a 'nucleus' triple is 'grown' by adding progressively further grains, to obtain a set of grains in which each triple is coherent. This is continued until a maximal such set is obtained.

6.2. Embedding approach

The embedding approach uses a suitable embedding $\mathbf{t}_2 : SO(3)/K_2 \rightarrow E$. Divisive cluster analysis is then applied to $\mathbf{t}_2([\mathbf{V}_1]_2), \ldots, \mathbf{t}_2([\mathbf{V}_n]_2)$ using

$$2 \left(\rho^2 - \langle \mathbf{t}_2([\mathbf{V}_i]_2), \mathbf{t}_2([\mathbf{V}_c]_2) \rangle \right) \tag{25}$$

as a measure of squared distance [see (5)] between $[\mathbf{V}_i]_2$ and the putative centre $[\mathbf{V}_c]_2$ of a cluster. The $[\mathbf{V}_c]_2$ for a cluster is chosen to minimize the sum of squared distances from that centre to the members of the cluster (*i.e.* it is set to be the sample mean defined in Section 3.1). If only one cluster is
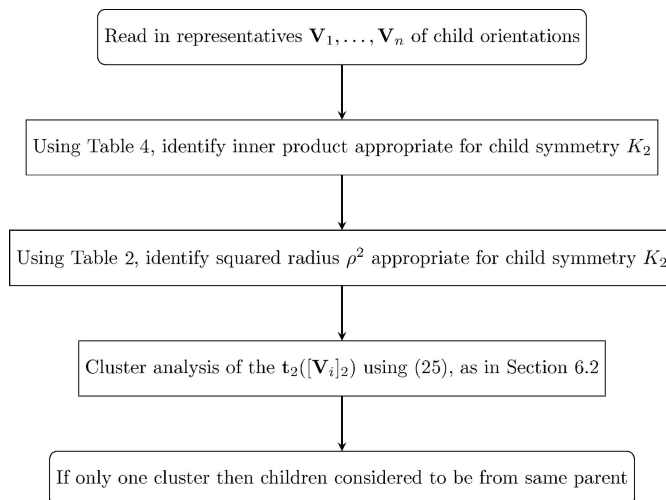
Figure 4
A flow chart for assessing common parentage.

found then it is considered that $[\mathbf{V}_1]_2, \ldots, [\mathbf{V}_n]_2$ arise from the same parent.

A flow chart for implementation of the technique described in this subsection is given in Fig. 4.

7. Reconstruction

In some contexts the orientations $[\mathbf{V}_1]_2, \ldots, [\mathbf{V}_n]_2$ of child crystals are observed but the parent crystals are not visible. The *reconstruction problem* is that of estimating the orientation $[\mathbf{U}]_1$ of the parent crystal, assuming a given orientational relationship of the form (1) with $\mathbf{R}$ and $[\mathbf{A}]_{1,2}$ known. Thus, the problem is to estimate $[\mathbf{U}]_1$ such that $[\mathbf{V}_i]_2$ is close to $[\mathbf{RW}_i\mathbf{A}]_2$ ($i = 1, \ldots, n$) for some $\mathbf{W}_1, \ldots, \mathbf{W}_n$ with $[\mathbf{W}_1]_1 = \cdots = [\mathbf{W}_n]_1 = [\mathbf{U}]_1$.

7.1. Established methods

The reconstruction method introduced by Humbert *et al.* (1994) is based on the fact that, if the pairs $([\mathbf{U}]_1, [\mathbf{V}_i]_2)$ and $([\mathbf{U}]_1, [\mathbf{V}_j]_2)$ each satisfy the orientation relationship (1) (at least approximately) then (14) holds. It follows that

$$[\mathbf{U}]_1 \simeq [\mathbf{R}^{-1}\mathbf{V}_i \widetilde{\mathbf{H}}_i^{-1} \mathbf{A}^{-1}]_1 \simeq [\mathbf{R}^{-1}\mathbf{V}_j \widetilde{\mathbf{H}}_j^{-1} \mathbf{A}^{-1}]_1. \tag{26}$$

If $\mathbf{R}$ and $\mathbf{A}$ are known then applying this method to the three pairs (i, j) obtained from three variants yields a unique value for $[\mathbf{U}]_1$. If observations on n variants are available then Humbert & Gey (2002) and Gey & Humbert (2003) recommend that the values of $[\mathbf{U}]_1$ given by the $\binom{n}{3}$ triples of variants be averaged. Note that averaging of rotations is not well defined.

7.2. Embedding approach

One reconstruction method using the embedding approach starts with a suitable embedding $\mathbf{t}_2$ of $SO(3)/K_2$ and known (or estimated) values of $\mathbf{R}$ and $[\mathbf{A}]_2$. It then calculates $\mathbf{W}_1, \ldots, \mathbf{W}_n$ by the $\widehat{\mathbf{W}}_1, \ldots, \widehat{\mathbf{W}}_n$ that maximize $\sum_{i=1}^{n} \langle \mathbf{t}_2([\mathbf{RW}_i\mathbf{A}]_2), \mathbf{t}_2([\mathbf{V}_i]_2) \rangle$, *i.e.* that maximize

$$\sum_{i=1}^{n} \left\langle \mathbf{t}_2([\mathbf{W}_i^{-1}\mathbf{R}^{-1}\mathbf{V}_i]_2), \mathbf{t}_2([\mathbf{A}]_2) \right\rangle \qquad (27)$$

over $\mathbf{W}_1, \ldots, \mathbf{W}_n$ satisfying $[\mathbf{W}_1]_1 = \cdots = [\mathbf{W}_n]_1$, and then estimates $[\mathbf{U}]_1$ by $[\widehat{\mathbf{W}}_1]_1$. In other words, the estimate of $[\mathbf{U}]_1$ is the element of $SO(3)/K_1$ corresponding to the $\mathbf{U}$ in $SO(3)$ that maximizes

$$\sum_{i=1}^{n} \max_{\mathbf{H}_i \in K_1} \left\langle \mathbf{t}_2([\mathbf{H}_i^{-1}\mathbf{U}^{-1}\mathbf{R}^{-1}\mathbf{V}_i]_2), \mathbf{t}_2([\mathbf{A}]_2) \right\rangle, \qquad (28)$$

where $\mathbf{A}$ is any representative in $SO(3)$ of $[\mathbf{A}]_{1,2}$. In (28) it can be assumed without loss of generality that $\mathbf{H}_1 = \mathbf{I}_3$, the identity.

Locating the maximum of (28) involves maximization over $SO(3) \times K_1^n$, so it may be useful to consider an alternative estimator which is easier to compute. The left-hand approximate equality in (14) gives

$$\mathbf{R}^{-1}\mathbf{V}_i\widetilde{\mathbf{H}}_i^{-1}\mathbf{A}^{-1} \simeq \mathbf{U}\mathbf{H}_i, \qquad (29)$$

and so

$$\mathbf{t}_1([\mathbf{R}^{-1}\mathbf{V}_i\widetilde{\mathbf{H}}_i^{-1}\mathbf{A}^{-1}]_1) \simeq \mathbf{t}_1([\mathbf{U}]_1) \qquad (30)$$

for any embedding $\mathbf{t}_1$ of $SO(3)/K_1$. Define $\overline{\mathbf{A}}^{-1}$ by

$$\overline{\mathbf{A}}^{-1} = |K_2|^{-1} \sum_{\widetilde{\mathbf{H}} \in K_2} \widetilde{\mathbf{H}}\mathbf{A}^{-1}. \qquad (31)$$

Then (30) gives

$$\mathbf{t}_1([\mathbf{U}]_1) \simeq \mathbf{t}_1([\mathbf{R}^{-1}\mathbf{V}_i\overline{\mathbf{A}}^{-1}]_1). \qquad (32)$$

Thus it is reasonable to estimate $[\mathbf{U}]_1$ by the sample mean (based on $\mathbf{t}_1$) of $[\mathbf{R}^{-1}\mathbf{V}_1\overline{\mathbf{A}}^{-1}]_1, \ldots, [\mathbf{R}^{-1}\mathbf{V}_n\overline{\mathbf{A}}^{-1}]_1$, *i.e.* the $[\mathbf{U}]_1$ that maximizes

$$\left\langle \mathbf{t}_1([\mathbf{U}]_1), \sum_{i=1}^{n} \mathbf{t}_1([\mathbf{R}^{-1}\mathbf{V}_i\overline{\mathbf{A}}^{-1}]_1) \right\rangle. \qquad (33)$$

A flow chart for implementation of the technique described in this subsection is given in Fig. 5.

Read in representatives $\mathbf{V}_1, \ldots, \mathbf{V}_n$ of child orientations

$\downarrow$

Using Table 1, identify embedding $\mathbf{t}_2$ appropriate for child symmetry K_2

$\downarrow$

Obtain $\bar{\mathbf{A}}^{-1}$ by (31)

$\downarrow$

Search for $\mathbf{U}$ in $SO(3)$ that maximizes (33)
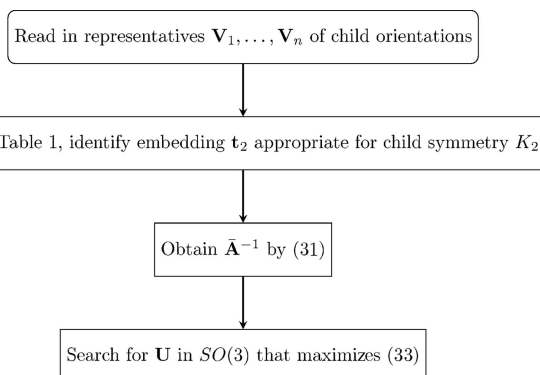
Figure 5
A flow chart for reconstruction of a parent.
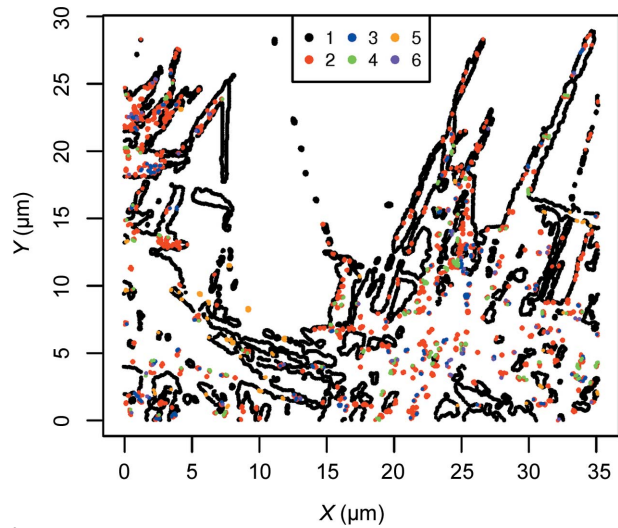
Figure 6
Locations of sites coloured by cluster.

(a)

(b)
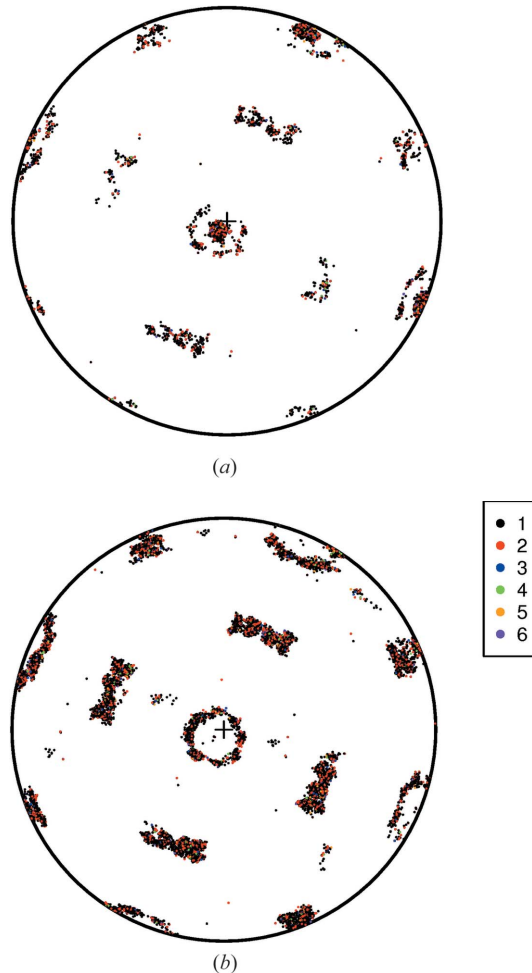
Figure 7
(a) A stereonet diagram showing the $n = 9707$ orientations $[\mathbf{U}_i]_1$, $i = 1, \ldots, n$, in the austenite phase from Wendler *et al.* (2017). (b) The corresponding martensite orientations $[\mathbf{V}_i]_2$, $i = 1, \ldots, n$.

8. Practical applications

8.1. Spatially varying orientation relationship: austenite–martensite transformation

The data set considered by Wendler *et al.* (2017) consists of 9707 pairs of orientations $([\mathbf{U}_i]_1, [\mathbf{V}_i]_2)$, $i = 1, \ldots, 9707$, of austenite and martensite, respectively. For each pair the orientations are measured at sites that are close but separated by a boundary between grains. The locations of the pairs on the surface of a steel sample are shown in Fig. 6. Fig. 7 displays these orientations on two stereonets (stereographic projections), one for the (face-centred cubic) austenite phase and the other for the (body-centred cubic) martensite phase. The symmetry groups K_1 and K_2 are both equal to the octahedral group O. In Fig. 7, each disc represents the upper half of the unit sphere, and each orientation $[\mathbf{U}_i]_1$ or $[\mathbf{V}_i]_2$ is represented by the three points at which the three (unordered) orthogonal axes determined by $[\mathbf{U}_i]_1$ or $[\mathbf{V}_i]_2$ intersect the upper half of the unit sphere. In each diagram there is considerable variation, which is due partly to the differing crystal orientations

$[\mathbf{U}_i]_1$ of the austenite phase prior to the transformation. However, there is a degree of clustering present, which can be explained by differing orientation relationships $[\mathbf{A}]_{1,2}$ among the pairs of observations.

A cluster analysis, as outlined in Section 5, using S_∞ from (8) [rather than S_2 from (7)] was carried out. It reveals six clusters in $O \backslash SO(3)/O$ of values $[\widehat{\mathbf{A}}_1]_{1,2}, \ldots, [\widehat{\mathbf{A}}_6]_{1,2}$ of $[\widehat{\mathbf{A}}]_{1,2}$. Most observations belong to cluster 1 ($n_1 = 7214$) or cluster 2 ($n_2 = 1844$). Note that this is not a spatial clustering but rather a clustering of common orientation relationships. The locations of the clusters are shown by the colouring of the symbols in Fig. 6, and all six clusters occur at locations spread all over the surface of the steel sample.

Fig. 8(*a*) shows the estimated orientations $[\widehat{\mathbf{A}}_c]_{1,2}$ for each of the six clusters, $c = 1, \ldots, 6$. These same orientations are shown together with the $[\mathbf{U}_i^{\mathrm{T}}\mathbf{V}_i]_{1,2}$ in Fig. 8(*b*). In drawing diagrams of this type we have had to make the choice to display each $[\widehat{\mathbf{A}}_c]_{1,2} \in O \backslash SO(3)/O$ as an element $[\widehat{\mathbf{A}}_c]_2$ of

(a)

(a)

(b)

(b)
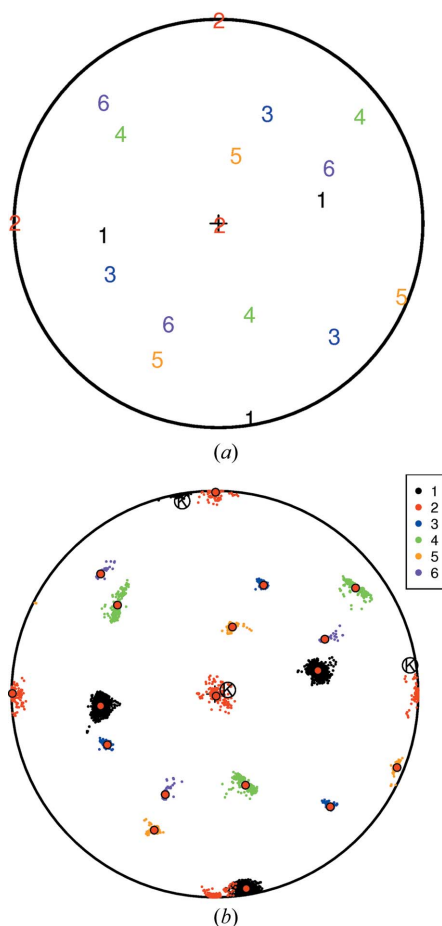
Figure 8
(*a*) Orientation relationships $[\widehat{\mathbf{A}}_c]_{1,2}$ in the six fitted clusters $c = 1, \ldots, 6$. The orientations are plotted as members of $SO(3)/K_2$ by (arbitrarily) selecting the element of $SO(3)/O$ for which $[\widehat{\mathbf{A}}_c]_2$ is closest to the first observation in each cluster: $[\mathbf{U}_{c1}^{\mathrm{T}}\mathbf{V}_{c1}]_2$. (*b*) Under the same convention as in panel (*a*), the data $[\mathbf{U}_i^{\mathrm{T}}\mathbf{V}_i]_{1,2}$ are shown, coloured by cluster. The fitted orientations $[\widehat{\mathbf{A}}]_{1,2}$ are shown as red filled circles.
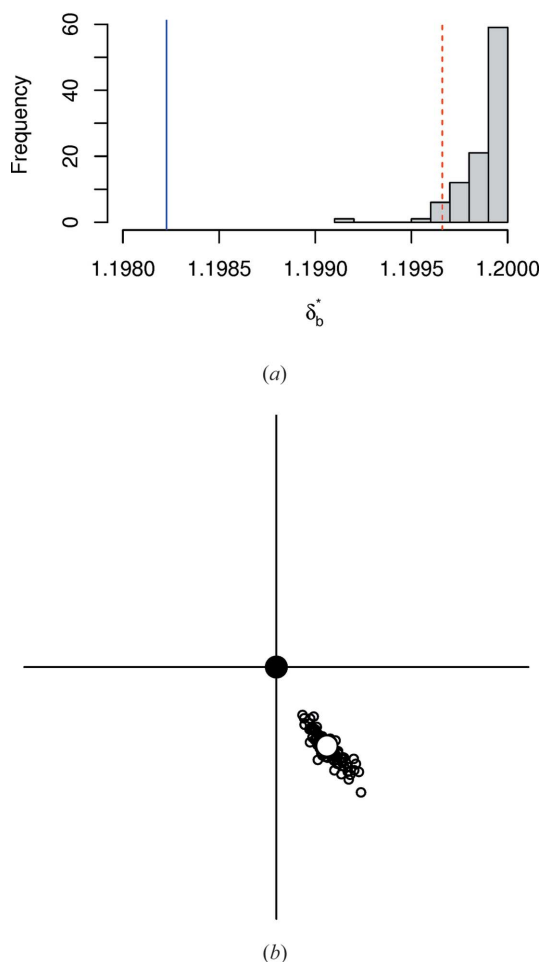
Figure 9
(*a*) A histogram of bootstrap $\{\delta([\widehat{\mathbf{A}}_b]_{1,2}, [\widehat{\mathbf{A}}]_{1,2})\}_{b=1}^B$ values. The limit c_α of the 95% confidence region is indicated by the red dashed line. The estimated δ value for the hypothesized value is the vertical solid blue line on the left-hand side. (*b*) Locations of bootstrap estimates on an enlarged stereonet. The estimate $[\widehat{\mathbf{A}}]_{1,2}$ is shown as the large open circle, the hypothesized value $[\mathbf{I}_3]_{1,2}$ as a filled circle at the origin, and the bootstrap estimates as small open circles. The large cross in (*b*) is the same size as the crosses at the centres of the stereonets in Figs. 7 and 8.

$SO(3)/O$, (arbitrarily) selecting the representation closest to the first observation $[\mathbf{U}_{c1}^{\mathrm{T}}\mathbf{V}_{c1}]_2$ in each cluster.

Fig. 7(b) appears to be a left–right reflection of the centre plot [labelled '{100}') in Fig. 5(d) of Wendler *et al.* (2017)]. (That the figures are not identical may be due to a difference in convention regarding Euler angles.) The colour codings in the two figures are completely different; that in Fig. 7(b) is derived from having taken full account of all ambiguities in rotation.

8.2. Testing whether $[A]_{1,2}$ has a given value

In the analysis in Section 8.1 the estimated orientation relationship $[\widehat{\mathbf{A}}]_{1,2}$ for cluster 2 is very close to the identity $\mathbf{I}_3$. We can test the hypothesis $H_0 : [\mathbf{A}]_{1,2} = [\mathbf{I}_3]_{1,2}$ by forming a bootstrap confidence region for $[\widehat{\mathbf{A}}]_{1,2}$ using the methods of Section 4. For demonstration purposes, we took a random subset of 50 observations from cluster 2. We then generated $B = 100$ bootstrap samples from this subset, and re-estimated $[\mathbf{A}]_{1,2}$ in each case. The distribution of values of $\{\delta([\widehat{\mathbf{A}}_b]_{1,2}, [\widehat{\mathbf{A}}]_{1,2})\}_{b=1}^{B}$ is shown in Fig. 9(a), and the similarity measure δ_0 for the hypothesized value falls well outside the distribution, a convincing rejection of H_0. Fig. 9(b) displays the original estimate $[\widehat{\mathbf{A}}]_{1,2}$ and the 100 replicate estimates, all lying well away from the hypothesized value $[\mathbf{I}_3]_{1,2}$.

9. Software

The analyses in Section 8 were performed using the freely available statistical software *R* (https://www.R-project.org/). A general and flexible MATLAB tool kit for the analysis of crystallographic data is provided by the open-source crystallographic toolbox *MTEX* (Bachmann *et al.*, 2010).

10. Conclusions

The intrinsic symmetries of crystal structures provide a challenge to statistical analysis due to the ambiguities of their representations. The challenge becomes greater in a setting where the orientations of crystals with different symmetries are to be compared.

In this paper we have applied the embedding approach from directional statistics to the representation of crystallographic orientation data. This approach enables us to reformulate standard problems of estimation and inference in the crystallographic setting, eliminating the ambiguities which arise from the crystallographic symmetries, while retaining the genuine multiplicity of crystallographic variants.

Although the embedded objects we work with may be unfamiliar, they are straightforward to implement in software, and should provide a practical tool for researchers seeking to characterize crystallographic structures and their transformations.

APPENDIX *A*
The number of variants

In the context of Section 2.3, elements $[\mathbf{UH}_i]_1$ and $[\mathbf{UH}_j]_1$ of $SO(3)/K_1$ give rise to the same element of $SO(3)/K_2$ under

orientation relationship (1) if and only if $[\mathbf{RUH}_i\mathbf{A}]_2 = [\mathbf{RUH}_j\mathbf{A}]_2$. Since

$$[\mathbf{RUH}_i\mathbf{A}]_2 = [\mathbf{RUH}_j\mathbf{A}]_2 \Leftrightarrow (\mathbf{RUH}_i\mathbf{A})^{-1}(\mathbf{RUH}_j\mathbf{A}) \in K_2$$
$$\Leftrightarrow \mathbf{A}^{-1}\mathbf{H}_i^{-1}\mathbf{H}_j\mathbf{A} \in K_2 \Leftrightarrow \mathbf{H}_i^{-1}\mathbf{H}_j \in K_1 \cap (\mathbf{A}K_2\mathbf{A}^{-1}) = K_{\mathbf{A}},$$
$$(34)$$

the number of variants is $s = |K_1|/|K_{\mathbf{A}}|$.

Proposition 1. There is a subset $\mathcal{B}$ of $SO(3)$ that has measure 0 and such that if $\mathbf{A}$ is outside $\mathcal{B}$ then $s = |K_1|$.

Proof. For given $\mathbf{H}_i$ in K_1 and $\tilde{\mathbf{H}}_j$ in K_2, define the set $\mathcal{B}_{ij}$ by

$$\mathcal{B}_{ij} = \{\mathbf{W} \in SO(3) : \mathbf{H}_i\mathbf{W} = \mathbf{W}\tilde{\mathbf{H}}_j\}. \quad (35)$$

Then either (i) $\mathcal{B}_{ij} = SO(3)$ or (ii) $\mathcal{B}_{ij}$ is contained in some proper subspace of the vector space of 3×3 matrices. In case (i), $\mathbf{H}_i\mathbf{W} = \mathbf{W}\tilde{\mathbf{H}}_j$ for all $\mathbf{W}$ in $SO(3)$, so that $\mathbf{H}_i = \tilde{\mathbf{H}}_j$ and therefore $\mathbf{H}_i\mathbf{W} = \mathbf{W}\mathbf{H}_i$ for all $\mathbf{W}$ (including $\mathbf{W} = \mathbf{I}_3$), implying that $\mathbf{H}_i = \mathbf{I}_3$. In case (ii), there is some $\mathbf{C}$ in $SO(3)$ such that $\mathrm{tr}(\mathbf{CW}) = 0$ for all $\mathbf{W}$ in $\mathcal{B}_{ij}$. Thus $\mathcal{B}_{ij}$ has measure 0. Now let $\mathbf{H}_i$ and $\tilde{\mathbf{H}}_j$ run through in K_1 and K_2, respectively and define $\mathcal{B}$ as

$$\mathcal{B} = \cup_{\mathcal{B}_{ij} \neq SO(3)} \mathcal{B}_{ij}. \quad (36)$$

Since this is a finite union, $\mathcal{B}$ has measure 0. If $\mathbf{H} \in K_{\mathbf{A}}$ then $\mathbf{H} = \mathbf{H}_i$ and $\mathbf{H} = \mathbf{A}\tilde{\mathbf{H}}_j\mathbf{A}^{-1}$ for some $\mathbf{H}_i$ in K_1 and $\tilde{\mathbf{H}}_j$ in K_2, so that $\mathbf{A} \in \mathcal{B}_{ij}$. Thus, if $\mathbf{A} \notin \mathcal{B}$ then $\mathbf{H} = \mathbf{I}_3$, so that $|K_{\mathbf{A}}| = 1$, and therefore $s = |K_1|$. □

It follows from Proposition 1 that if $\mathbf{A}$ is chosen randomly from some continuous distribution then, with probability 1, $s = |K_1|$.

APPENDIX *B*
Some embeddings of $SO(3)/K$

The embedding approach is based on embeddings, *i.e.* well defined equivariant one-to-one functions $\mathbf{t}_K : SO(3)/K \rightarrow E$, where E is an inner-product space on which $SO(3)$ acts, such that $\mathbf{t}_K([\mathbf{U}])$ has expectation 0 if $[\mathbf{U}]$ is uniformly distributed on $SO(3)/K$. Here, we focus on a simple choice of embedding $\mathbf{t}_K$ of $SO(3)/K$ into an appropriate space of symmetric arrays, where K is one of the crystallographic groups C_1, C_2, C_3, C_4, D_2, D_6 and O or the tetrahedral group T (in Schoenflies notation). Appropriate embeddings $\mathbf{t}_K$ for general point groups K of the first kind are considered by Arnold & Jupp (2019) and Arnold *et al.* (2018, 2021).

It is convenient to describe the orientation of a crystal by a frame, meaning a set of vectors or axes that are fixed in the crystal. The presence of symmetry under group K means that such a frame is equivalent to one obtained from it by a rotation in K. The equivalence classes are known as K-frames. For $K = C_1$ the frame is taken to be $(\mathbf{u}_1, \mathbf{u}_2, \mathbf{u}_3)$ with $\mathbf{u}_1$, $\mathbf{u}_2$, $\mathbf{u}_3$ orthogonal unit vectors; for $K = C_2$ the frame is $(\mathbf{u}_0, \pm\mathbf{u}_1)$ with $\mathbf{u}_0$ a unit vector and $\pm\mathbf{u}_1$ an axis orthogonal to $\mathbf{u}_0$; for $K = D_2$ it is a pair of orthogonal axes $(\pm\mathbf{u}_1, \pm\mathbf{u}_2)$; for $K = C_r$ with $r \geq 3$ or $K = D_6$ with $r \geq 3$, the vectors $(\mathbf{u}_1, \ldots, \mathbf{u}_r)$ are unit normals

Table 3
Symmetry groups and frames.

The $\mathbf{u}_i$ are unit vectors. $|K|$ is the number of elements in K.

Group, K	Name	$|K|$	Frame	Notes
C_1	Trivial	1	$(\mathbf{u}_1, \mathbf{u}_2, \mathbf{u}_3)$	$\mathbf{u}_1, \mathbf{u}_2, \mathbf{u}_3$ orthonormal, $\mathbf{u}_3 = \mathbf{u}_1 \times \mathbf{u}_2$
C_2	Cyclic	2	$(\mathbf{u}_0, \pm\mathbf{u}_1)$	$\mathbf{u}_0, \mathbf{u}_1$ orthonormal
$C_r\ (r \geq 3)$	Cyclic	r	$(\mathbf{u}_1, \ldots, \mathbf{u}_r)$	$\mathbf{u}_1, \ldots, \mathbf{u}_r$ coplanar, known up to cyclic order, $\mathbf{u}_i^T\mathbf{u}_{i-1} = \cos(2\pi/r)$ for $i = 2, \ldots, r$
D_2	Dihedral	4	$(\pm\mathbf{u}_1, \pm\mathbf{u}_2)$	Orthogonal axes
D_6	Dihedral	12	$(\mathbf{u}_1, \ldots, \mathbf{u}_6)$	$\mathbf{u}_1, \ldots, \mathbf{u}_6$ coplanar, known up to cyclic order and reversal, $\mathbf{u}_i^T\mathbf{u}_{i-1} = \cos(\pi/3)$ for $i = 2, \ldots, 6$
T	Tetrahedral	12	$\{\mathbf{u}_1, \ldots, \mathbf{u}_4\}$	$\mathbf{u}_i^T\mathbf{u}_j = -1/3$ for $i \neq j$
O	Octahedral = cubic	24	$\{\pm\mathbf{u}_1, \pm\mathbf{u}_2, \pm\mathbf{u}_3\}$	Orthogonal axes

to the sides of a regular r-gon or hexagon; for O and T, the axes $(\pm\mathbf{u}_1, \pm\mathbf{u}_2, \pm\mathbf{u}_3)$ and $(\pm\mathbf{u}_1, \pm\mathbf{u}_2, \pm\mathbf{u}_3, \pm\mathbf{u}_4)$ are unit normals to the sides of the cubic crystal and tetrahedral crystal, respectively. The K-frames will be denoted by square brackets, *e.g.* for $K = C_r$ $[\mathbf{u}_1, \ldots, \mathbf{u}_r]$ denotes the K-frame arising from $(\mathbf{u}_1, \ldots, \mathbf{u}_r)$. The frames used are listed in Table 3. Note that the frames are specified entirely by vectors and axes; they do not depend on any coordinate system. For notational simplicity, we shall sometimes denote a K-frame by $[\mathbf{U}]$.

The embeddings $\mathbf{t}_K$ are given explicitly in Table 1. They are based on symmetric r-way arrays, $\otimes^r\mathbf{u}_i$, which can be thought of as rth powers of vectors. In mathematical terms, they are coordinate representations of r-fold tensor products. For vectors $\mathbf{u}_1, \ldots, \mathbf{u}_r$ with $\mathbf{u}_i = (u_{i,1}, u_{i,2}, u_{i,3})^T$ for $i = 1, \ldots, r$, the r-way array $\otimes^r\mathbf{u}_i$ has $(j_1, \ldots, j_r)$th entry

$$(\otimes^r\mathbf{u}_i)_{j_1, \ldots, j_r} = \prod_{k=1}^{r} u_{i,j_k}, \quad 1 \leq j_1, \ldots, j_r \leq 3, \quad (37)$$

e.g. $\otimes^2\mathbf{u}_i = \mathbf{u}_i\mathbf{u}_i^T$. Some of the $\mathbf{t}_K$ also involve the arrays $\mathbf{N}_r$ for r even. These symmetric r tensors are defined by

$$\langle \mathbf{N}_r, \otimes^r\mathbf{v} \rangle = \|\mathbf{v}\|^r \quad \mathbf{v} \in \mathbb{R}^3, \quad (38)$$

where $\|\mathbf{v}\|$ denotes the length of $\mathbf{v}$. In coordinate terms they have entries

$$(\mathbf{N}_r)_{j_1, \ldots, j_r} = \frac{1}{r!} \sum_{\sigma \in \Sigma_r} \prod_{i=1}^{r/2} \delta_{\sigma(j_{2i-1})\sigma(j_{2i})}, \quad (39)$$

where Σ_r is the group of permutations of $\{1, \ldots, r\}$ and $\delta_{ij} = 1$ for $i = j$, $\delta_{ij} = 0$ otherwise. Thus, *e.g.* $(\mathbf{N}_4)_{j_1, j_2, j_3, j_4} = (\delta_{j_1 j_2}\delta_{j_3 j_4} + \delta_{j_1 j_3}\delta_{j_2 j_4} + \delta_{j_1 j_4}\delta_{j_2 j_3})/3$. Some of the embeddings involve subtraction of constant terms to ensure that $E\{\mathbf{t}_K([\mathbf{U}])\} = 0$ under uniformity. In the case of C_r, the embeddings contain oriented vectors $\mathbf{u}_0$ to specify the orientation of the directed axis of symmetry.

For our purposes it is not necessary to construct the representations $\mathbf{t}_K([\mathbf{U}])$ explicitly; it is sufficient to compute inner products $\langle \mathbf{t}_K([\mathbf{U}]), \mathbf{t}_K([\mathbf{V}]) \rangle$ as required, where $\langle \cdot, \cdot \rangle$ is the standard inner product on the relevant space of symmetric arrays. The inner products are listed in Table 4.

Some much more general classes of embeddings than the $\mathbf{t}_K$ given in Table 1 are considered by Hielscher & Lippert (2021) and Arnold *et al.* (2021).

In general, it is simpler and computationally faster to use inner products than to use misorientation angles. This is illu-

Table 4
Inner products of transforms of symmetric frames.

For C_r with $r \geq 3$, $\mathbf{u}_0 = \{\sin(2\pi/r)\}^{-1} \mathbf{u}_1 \times \mathbf{u}_2$. For D_2, $\mathbf{u}_3 = \pm\mathbf{u}_1 \times \mathbf{u}_2$.

Group, K	Inner product
C_1	$\langle \mathbf{t}_{C_1}(\mathbf{u}_1, \mathbf{u}_2, \mathbf{u}_3), \mathbf{t}_{C_1}(\mathbf{v}_1, \mathbf{v}_2, \mathbf{v}_3) \rangle = \mathbf{u}_1^T\mathbf{v}_1 + \mathbf{u}_2^T\mathbf{v}_2 + \mathbf{u}_3^T\mathbf{v}_3$
C_2	$\langle \mathbf{t}_{C_2}(\mathbf{u}_0, \pm\mathbf{u}_1), \mathbf{t}_{C_2}(\mathbf{v}_0, \pm\mathbf{v}_1) \rangle = \mathbf{u}_0^T\mathbf{v}_0 + (\mathbf{u}_1^T\mathbf{v}_1)^2 - 1/3$
C_3	$\langle \mathbf{t}_{C_3}([\mathbf{u}_1, \ldots, \mathbf{u}_3]), \mathbf{t}_{C_3}([\mathbf{v}_1, \ldots, \mathbf{v}_3]) \rangle = \mathbf{u}_0^T\mathbf{v}_0 + \sum_{i=1}^{3}\sum_{j=1}^{3} (\mathbf{u}_i^T\mathbf{v}_j)^3$
C_4	$\langle \mathbf{t}_{C_4}([\mathbf{u}_1, \ldots, \mathbf{u}_4]), \mathbf{t}_{C_4}([\mathbf{v}_1, \ldots, \mathbf{v}_4]) \rangle = \mathbf{u}_0^T\mathbf{v}_0 + \sum_{i=1}^{4}\sum_{j=1}^{4} (\mathbf{u}_i^T\mathbf{v}_j)^4 - 16/5$
D_2	$\langle \mathbf{t}_{D_2}(\pm\mathbf{u}_1, \pm\mathbf{u}_2), \mathbf{t}_{D_2}(\pm\mathbf{v}_1, \pm\mathbf{v}_2) \rangle = (\mathbf{u}_1^T\mathbf{v}_1)^2 + (\mathbf{u}_2^T\mathbf{v}_2)^2 + (\mathbf{u}_3^T\mathbf{v}_3)^2 - 1$
D_4	$\langle \mathbf{t}_{D_4}([\mathbf{u}_1, \ldots, \mathbf{u}_4]), \mathbf{t}_{D_4}([\mathbf{v}_1, \ldots, \mathbf{v}_4]) \rangle = \sum_{i=1}^{4}\sum_{j=1}^{4} (\mathbf{u}_i^T\mathbf{v}_j)^4 - 16/5$
D_6	$\langle \mathbf{t}_{D_6}([\mathbf{u}_1, \ldots, \mathbf{u}_6]), \mathbf{t}_{D_6}([\mathbf{v}_1, \ldots, \mathbf{v}_6]) \rangle = \sum_{i=1}^{6}\sum_{j=1}^{6} (\mathbf{u}_i^T\mathbf{v}_j)^6 - 36/7$
T	$\langle \mathbf{t}_T(\{\mathbf{u}_1, \mathbf{u}_2, \mathbf{u}_3, \mathbf{u}_4\}), \mathbf{t}_T(\{\mathbf{v}_1, \mathbf{v}_2, \mathbf{v}_3, \mathbf{v}_4\}) \rangle = \sum_{i=1}^{4}\sum_{j=1}^{4} (\mathbf{u}_i^T\mathbf{v}_j)^3$
O	$\langle \mathbf{t}_O(\{\pm\mathbf{u}_1, \pm\mathbf{u}_2, \pm\mathbf{u}_3\}), \mathbf{t}_O(\{\pm\mathbf{v}_1, \pm\mathbf{v}_2, \pm\mathbf{v}_3\}) \rangle = \sum_{i=1}^{3}\sum_{j=1}^{3} (\mathbf{u}_i^T\mathbf{v}_j)^4 - 9/5$

strated neatly in the cubic case. Consider $[\mathbf{U}]$ and $[\mathbf{V}]$ in $SO(3)/O$ with $\mathbf{u}_1, \mathbf{u}_2, \mathbf{u}_3$ and $\mathbf{v}_1, \mathbf{v}_2, \mathbf{v}_3$ as the columns of $\mathbf{U}$ and $\mathbf{V}$, respectively. Then

$$\langle \mathbf{t}_O([\mathbf{U}]), \mathbf{t}_O([\mathbf{V}]) \rangle = \sum_{i=1}^{3}\sum_{j=1}^{3} (\mathbf{u}_i^T\mathbf{v}_j)^4 - 9/5, \quad (40)$$

whereas the misorientation angle is

$$\min \arccos\{(\epsilon_1\mathbf{u}_1^T\mathbf{v}_j + \epsilon_2\mathbf{u}_2^T\mathbf{v}_k + \epsilon_3\mathbf{u}_3^T\mathbf{v}_\ell - 1)/2\}, \quad (41)$$

the minimum being over all $\epsilon_1, \epsilon_2, \epsilon_3 = \pm 1$ and all permutations j, k, ℓ of 1, 2, 3. Evaluating (41) involves about six times as many operations as evaluating (40).

research papers

References

Abbasi, M., Kim, D.-I., Nelson, T. W. & Abbasi, M. (2014). *Mater. Charact.* **95**, 219–231.

Abbasi, M., Nelson, T. W., Sorensen, C. D. & Wei, L. (2012). *Mater. Charact.* **66**, 1–8.

Arnold, R. & Jupp, P. E. (2019). *Applied Directional Statistics: Modern Methods and Case Studies*, edited by C. Ley & T. Verdebout, pp. 41–60. London: Chapman & Hall/CRC.

Arnold, R., Jupp, P. E. & Schaeben, H. (2018). *J. Multivariate Anal.* **165**, 73–85.

Arnold, R., Jupp, P. E. & Schaeben, H. (2021). *Directional Statistics for Innovative Applications*, edited by A. SenGupta & B. C. Arnold. Heidelberg: Springer.

Bachmann, F., Hielscher, R. & Schaeben, H. (2010). *Solid State Phenom.* **160**, 63–68.

Cayron, C. (2006). *Acta Cryst.* A**62**, 21–40.

Cayron, C. (2016). *Acta Mater.* **111**, 417–441.

Cayron, C. (2019). *Acta Cryst.* A**75**, 411–437.

Cayron, C., Artaud, B. & Briottet, L. (2006). *Mater. Charact.* **57**, 386–401.

Everitt, B., Landau, S., Leese, M. & Stahl, D. (2011). *Cluster Analysis*, 5th ed. *Wiley Series in Probability and Statistics*. Chichester: John Wiley and Sons.

Gey, N. & Humbert, M. (2003). *J. Mater. Sci.* **38**, 1289–1294.

Gomes de Araujo, E., Pirgazi, H., Sanjari, M., Mohammadi, M. & Kestens, L. A. I. (2021). *J. Appl. Cryst.* **54**, 569–579.

Hielscher, R. & Lippert, L. (2021). *J. Multivariate Anal.* **185**, 104764.

Humbert, M., Germain, L., Gey, N. & Boucard, E. (2015). *Acta Mater.* **82**, 137–144.

Humbert, M. & Gey, N. (2002). *J. Appl. Cryst.* **35**, 401–405.

Humbert, M., Moustahfid, H., Wagner, F. & Philippe, M. J. (1994). *Scr. Metall. Mater.* **30**, 377–382.

Humbert, M., Wagner, F., Moustahfid, H. & Esling, C. (1995). *J. Appl. Cryst.* **28**, 571–576.

Johnstone, D. N., Martineau, B. H., Crout, P., Midgley, P. A. & Eggeman, A. S. (2020). *J. Appl. Cryst.* **53**, 1293–1298.

Karthikeyan, T., Saroja, S. & Vijayalakshmi, M. (2006). *Scr. Mater.* **55**, 771–774.

Kitahara, H., Ueji, R., Tsuji, N. & Minamino, Y. (2006). *Acta Mater.* **54**, 1279–1288.

Koumatos, K. & Muehlemann, A. (2017). *Acta Cryst.* A**73**, 115–123.

Kurdjumow, G. & Sachs, G. (1930). *Z. Phys.* **64**, 325–343.

Mackenzie, J. K. (1957). *Acta Cryst.* **10**, 61–62.

Mainprice, D., Humbert, M. & Wagner, F. (1990). *Tectonophysics*, **180**, 213–228.

Mardia, K. V. & Jupp, P. E. (2000). *Directional Statistics*. Chichester: Wiley.

Miyamoto, G., Takayama, N. & Furuhara, T. (2009). *Scr. Mater.* **60**, 1113–1116.

Morales, L. F. G., Mainprice, D. & Kern, H. (2018). *Tectonophysics*, **724–725**, 93–115.

Morawiec, A. (2004). *Orientations and Rotations*, 1st ed. Berlin: Springer-Verlag.

Nishiyama, Z. (1934). *Sci. Rep. Tohoku Univ.* **23**, 637–664.

Nolze, G. (2004a). *Proceedings of the CHANNEL Users Conference 2004*, Ribe, Denmark, pp. 37–45. Berlin: BAM.

Nolze, G. (2004b). *Z. Metallkd.* **95**, 744–755.

Nolze, G. (2005). *Determining the f.c.c./b.c.c. Orientational Relationship in Plessite Regions of Iron Meteorites*. HKL Users Meeting.

Nolze, G. (2008). *Cryst. Res. Technol.* **43**, 61–73.

Nyyssönen, T., Isakov, M., Peura, P. & Kuokkala, V.-T. (2016). *Metall. Mater. Trans. A*, **47**, 2587–2590.

Nyyssönen, T., Peura, P. & Kuokkala, V.-T. (2018). *Metall. Mater. Trans. A*, **49**, 6426–6441.

Ostapovich, K. V. & Trusov, P. (2021). *Crystals*, **11**, 336.

Pitsch, W. (1959). *Philos. Mag.* **4**, 577–584.

Pitsch, W. (1967). *Arch. Eisenhüttenwesen* **38**, 853–864.

Wassermann, G. (1933). *Arch. Eisenhüttenwesen* **6**, 347–351.

Wassermann, G. (1935). *Über den Mechanismus der α–γ Umwandlung des Eisens. Mitteilungen aus dem Kaiser-Wilhelm-Institut für Eisenforschung zu Düsseldorf*. Düsseldorf: Verlag Stahleisen.

Wendler, M., Ullrich, C., Hauser, M., Krüger, L., Volkova, O., Weiß, A. & Mola, J. (2017). *Acta Mater.* **133**, 346–355.